

# Patient dose evaluation for the whole-body low-dose multidetector CT (WBLDMDCT) skeleton study in multiple myeloma (MM)

Fabiola Cretti<sup>1</sup>  · Giovanna Perugini<sup>2</sup>

Received: 2 March 2015 / Accepted: 23 July 2015 / Published online: 19 August 2015  
© Italian Society of Medical Radiology 2015

## Abstract

**Objective** This study aimed at estimating the patient effective dose during whole-body low-dose multi detector computed tomography with a scanner Philips Brilliance 64, and to compare it with those reported in literature for the same procedure and with the dose of the conventional X-ray examination in our institution.

**Materials and methods** WBLDMDCT effective dose was evaluated for 29 MM patients, using Dose Length Product values. Conventional X-ray examination dose was estimated using a Rando Phantom and Dose Area Product indexes. ICRP Publication 103 based coefficients were used.

**Results** Mean WBLDMDCT effective dose values—estimated using sex-specific conversion coefficients and body weight factors—were 3.6 and 2.8 mSv for females and males, respectively. The effective dose for the conventional method was 1.2 mSv for Rando phantom.

**Conclusion** The WBLDMDCT effective dose in our institution is consistent with the values reported in previous studies. Such a dose is about 2.5– to 3-fold higher than the mean radiation dose of the conventional X-ray study. Nevertheless, considering the improved diagnostic accuracy of the CT investigation, the comfort of the patient and the old age of the MM population, dose/quality ratio can be considered favourable.

**Keywords** Computed tomography patient dose · Whole-body low-dose multidetector CT (WBLDMDCT) · Multiple myeloma (MM) · Skeleton X-ray conventional examination

## Introduction

Multiple myeloma (MM) is the most common malignant primary bone tumour. It affects mainly elderly population with a peak of incidence in the seventh–eighth decade. Bone marrow aspiration or, preferably, biopsy is necessary for the diagnosis. The clinical staging, which is critical for prognosis and therapeutic planning, is based upon laboratory findings and radiological assessment of bone involvement [1–3].

Skeletal conventional X-ray imaging still represents the “gold standard” due to its wide availability and its low cost. However, it has been demonstrated that the X-ray imaging sensitivity is low, especially in detecting small bone lesions.

Furthermore, owing to the long acquisition time (about 30 min) and the necessity of continuously changing and uncomfortable positions, the X-ray examination is not well tolerated by elderly patients with bone pain.

First, Horger in 2007 settled a whole-body low-dose multidetector computed tomography (WBLDMDCT) [4] protocol: he showed that, given the high intrinsic contrast of bone tissue, even a low-dose protocol (40 mAs) produces images of good quality, suitable for diagnosis, with a significant radiation dose saving comparing with a standard CT protocol (4.1 mSv at 40 mAs versus 25.5 mSv at 250 mAs). The mean dose of the conventional X-ray study was 2.4 mSv [4, 5].

✉ Fabiola Cretti  
fabiolacretti@gmail.com; fcretti@hpg23.it

<sup>1</sup> USC Fisica Sanitaria, Imaging Department, Azienda Ospedaliera Papa Giovanni XXIII, Piazza OMS 1, 24100 Bergamo, Italy

<sup>2</sup> USC Radiologia, Imaging Department, Azienda Ospedaliera Papa Giovanni XXIII, Piazza OMS 1, 24100 Bergamo, Italy

**Table 1** Scan parameters set in the WBLDMDCT protocol

	Scan parameters
kV	120/140
mAs/rotation	40
Pitch	0.984
FOV/Matrix	500 mm/512
Detectors configuration	64 × 0.625 (8 × 5 mm)
Slice thickness/step	5 mm/5 mm
Reconstructed slice thickness	1.5 mm
Filter	Standard
Dose reduction methods	IR iDose (no automatic control of exposure)

Since then, the WBLDMDCT protocol has become more widespread in the clinical practice and several studies have proved that the sensitivity and specificity of the method are considerably superior to the conventional X-ray study [6, 7]. An advantage of the technique is also the possibility to evaluate the extrasosseous localization of the disease.

According to this new evidence, since August 2013 we agreed with haematologists at our institution to replace skeletal conventional X-ray examinations with WBLDMDCT in MM patients. We decided to evaluate the radiation dose of the first 29 consecutive patients with a biopsy-proven diagnosis of MM who underwent WBLDMDCT in our institution and to compare it with both the dose levels reported by literature for this protocol and the dose of the conventional X-ray study.

This is in compliance with the local Decree Law, (DL 187/2000) [8], that acknowledges the European Directive 97/43/EURATOM concerning radiological protection of persons against risks related to medical exposures. Such a document contemplates monitoring and optimization of patients' exposures and indicates quality tests of the equipment that have to satisfy acceptance criteria, and Diagnostic Reference Levels (DRL) checks as operative means to achieve optimization. An important upgrade of both the acceptance criteria and LDR is represented by the document RP 162 published in 2012 [9] that accounts for the technological evolution of the equipment and dedicates an important section also to the CT scanners. For the procedures where a DRL is not defined, it is suitable to refer to literature. Previous works concerning radiological evaluation of MM patients report radiation doses of about 4 mSv for the WBLDMDCT protocol and about 2 mSv for the conventional X-ray examination. The WBLDMDCT protocol, recently adopted in our institution, takes advantage not only of the high intrinsic contrast of the bone tissue, but also of the use of iterative reconstruction algorithms (IR). Such a reconstruction technique, recently introduced

in CT modality [10–12] as an alternative to conventional methods based on the filtered back projection (FBP), is able to reduce the noise (denoising) acting in the image space. As a consequence it is possible to obtain images with a signal to noise ratio (SNR) equivalent to those that would be obtained using FBP, but with a lower patient dose, or images with a lower level of noise at the same patient dose. The last option is the one of interest in the present study. A further value of these algorithms is the ability to uncouple the image noise from the modulation transfer function (MTF) properties so that the spatial resolution is preserved.

Given this context, in the present work, the dose to patient is evaluated for both the new CT protocol and the old conventional one. In the following paragraphs the dose indexes used for CT and conventional X-ray dosimetry are introduced. These physical quantities cannot be compared directly, but they can be used to estimate the effective dose, which is a radioprotection index relating to stochastic risk, that allows for the two methods to be compared.

## Materials and methods

### CT modality

#### *CT subjects and scan parameters*

The study was done for the first 29 patients with MM (14 males, 15 females, age  $67 \pm 13$  years, mean  $\pm$  standard deviation) who were examined with WBLDMDCT protocol in our department, using the CT scanner 64 Brilliance, Philips Medical System. The patients were positioned supine, with their arm over the head. A survey scan was performed to set the initial and end points of the diagnostic scan, with the parameters of acquisition and reconstruction shown in Table 1. The scan length was such that humera, head, neck, torso and femura were included, as shown in Fig. 1A-a.

#### *CT dose index*

The dose descriptor used in CT modality is the Computed Tomographic Dose Index (CTDI) [13], defined by the following expression:

$$\text{CTDI} = \frac{1}{nT} \int_{z_1}^{z_2} D(z) dz,$$

where  $D(z)$  is the radiation dose profile along the  $z$  axis,  $z_1$  and  $z_2$  are the limits of integration,  $n$  is the number of

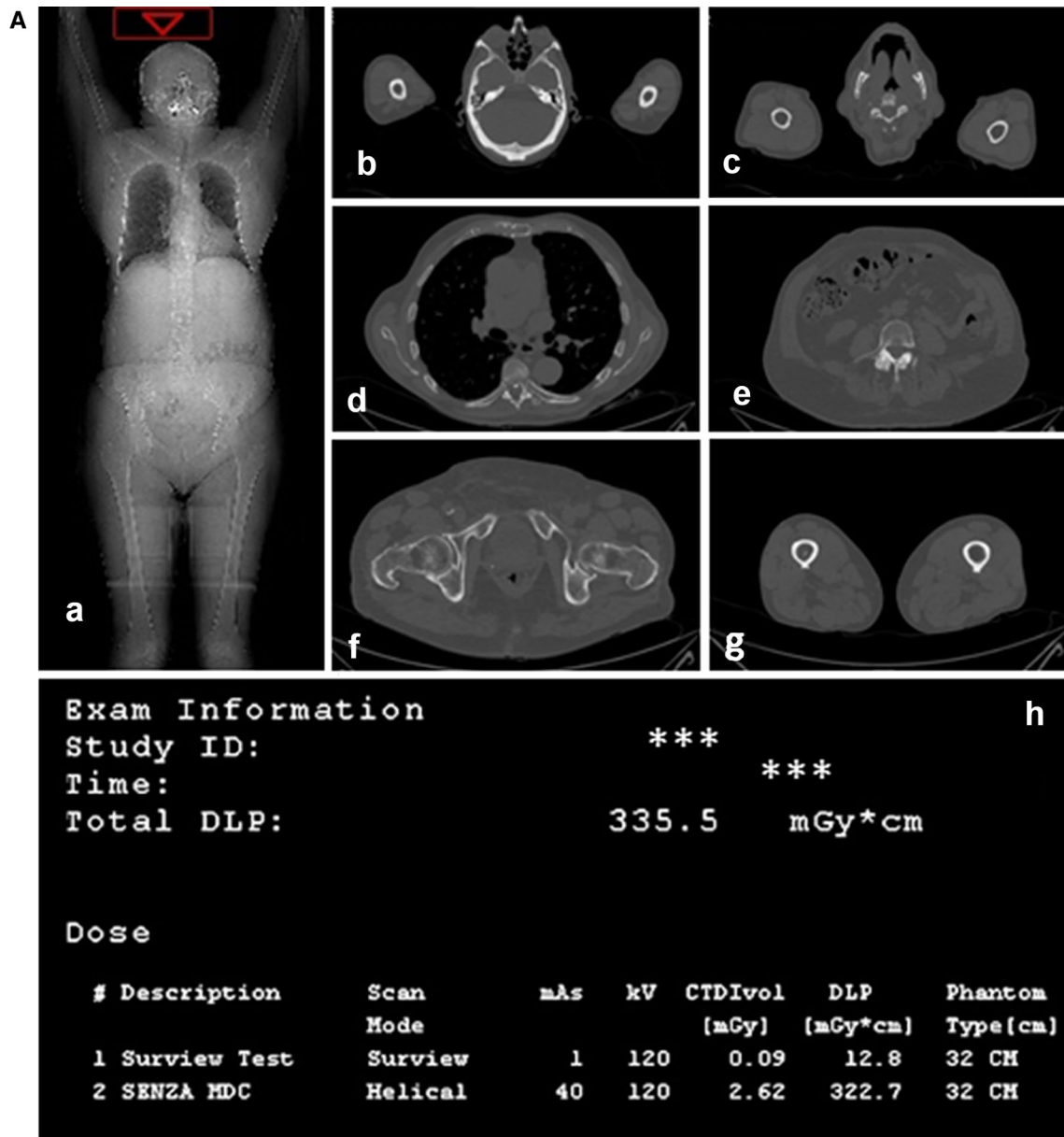


**Fig. 1** **A** The survey image used to plan the scan (a), an axial image for each of the segments investigated, including head and humera (b), neck (c), chest (d), abdomen (e), pelvis (f), femura (g) and finally the dose report (h). **B** Some images of the Rando phantom used to simu-

late the conventional examination of the skeleton: (i) anterior–posterior skull, (l) lateral skull; (m) pelvis; (n) ribs; (o) anterior–posterior dorsal and lumbar spine; (p) lateral spine

slices acquired simultaneously and  $T$  is the nominal slice thickness so that  $n \times T$  accounts for the beam width. This physical quantity is measured during a single axial scan of acrylic cylindrical phantoms with diameters of 16 or 32 cm, simulating head or body geometries, respectively. The measurements are taken at the centre (C) and at peripheral positions (P) of the phantom so that the weighted CTDI ( $CTDI_w$ ) can be estimated ( $CTDI_w = 1/3 CTDI_C + 2/3 CTDI_P$ ) representing the average CTDI across the irradiated slab (unit mGy).  $Z1$  and  $z2$  are

constrained by the length of the pencil beam ionization chamber (100 mm).

If the elicoidal technique is used, the volume dose index is considered, defined as  $CTDI_{vol} = CTDI_w/pitch$ , where the pitch is the ratio  $\Delta S/nT$ ,  $\Delta S$  being the table movement during a rotation of the X-ray tube.

In order to account for the extension of the irradiated volume, the dose length product (DLP [mGy × cm]) is considered, defined as  $DLP = CTDI_{vol} \times L_{scan}$ , where  $L_{scan}$  is the scan length.

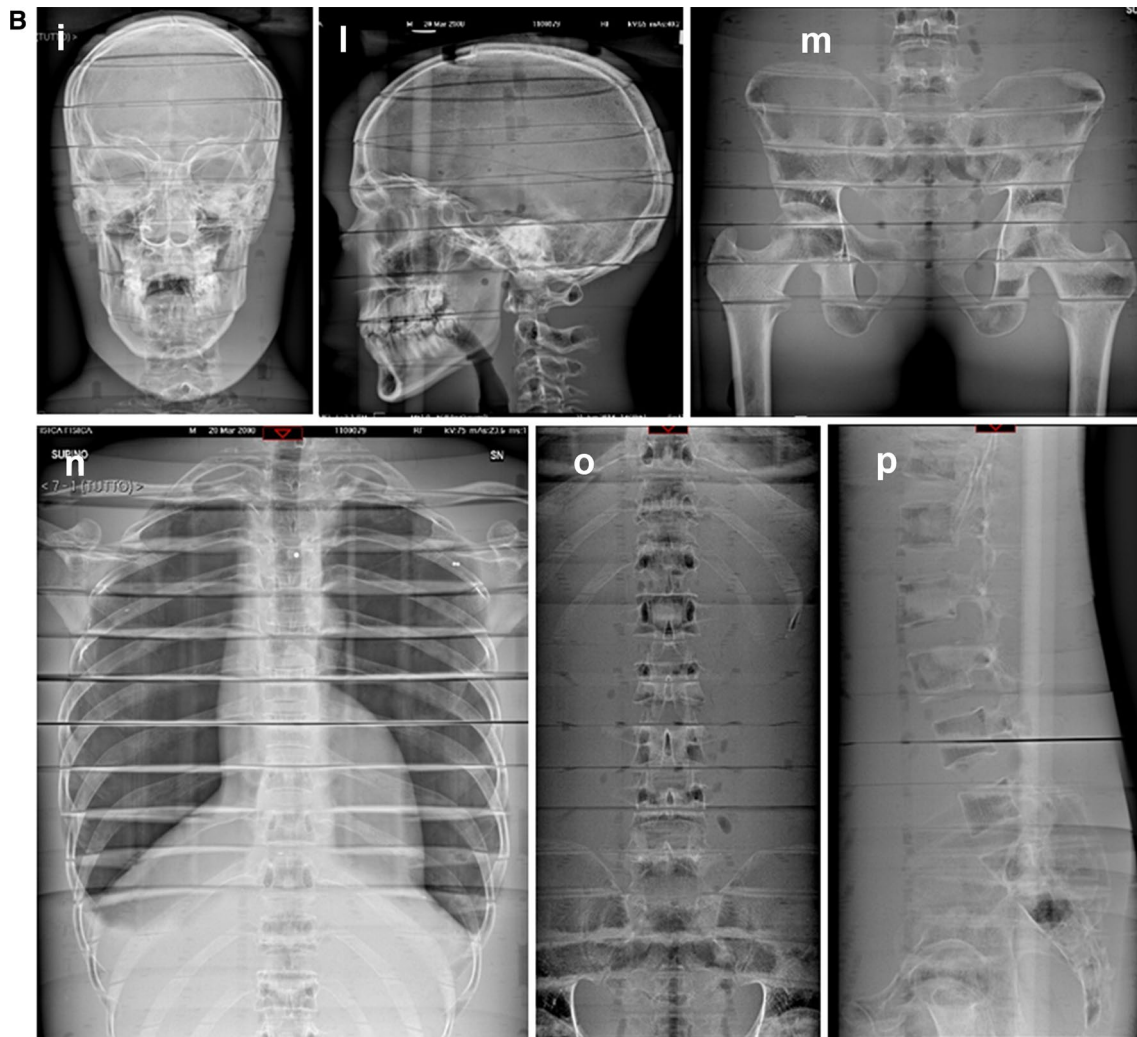


**Fig. 1** continued

### CT effective dose evaluation

The effective dose  $E$  is defined as  $E = \sum_T w_T H_T$  (expressed in millisievert  $mSv$ ) [14, 15].

$H_T$  being the equivalent dose in tissue or organ, and  $w_T$  being the appropriate tissue weighting factor; the equivalent dose in tissue or organ is given by  $H_T = D_m \times W_R$ , where  $D_m$  is the absorbed dose averaged in that tissue or organ (due to radiation  $R$ ), multiplied by the radiation weighting factor  $W_R$  (for photons  $W_R$  is equal to 1 for all energies).

Nevertheless,  $E$  can be easily estimated by multiplying the DLP values by conversion coefficients reported in literature for different body regions, obtained by means of Monte Carlo simulations and anthropomorphic phantoms [14, 16–19]. As during the CT procedure here considered different body segments are irradiated, the effective dose can be written as the sum

$$\sum_R DLP_R \times \left( \frac{E}{DLP} \right)_R,$$

where  $DLP_R$  is the DLP relative to the anatomic segment  $R$  and  $(E/DLP)_R$  is the DLP-to- $E$  conversion coefficient for the segment  $R$  (it represents the effective dose per unit DLP of the irradiated region).

For each patient in our study the following segments ( $R$ ) were included: head, neck, chest, abdomen, pelvis, humera and femura. The  $DLP_R$  of each single segment has been calculated as a fraction of the total DLP ( $DLP_{tot}$ ), the fraction being equal to the ratio  $\frac{L_R}{L_{tot}}$  ( $DLP_R = \frac{L_R}{L_{tot}} \times DLP_{tot}$ , where  $L_R$  is the length of the segment  $R$  and  $L_{tot}$  is the total scan length). The longitudinal extension of each segment was measured using the survey scan. For each segment  $R$  the contribution to the effective dose has been calculated using the pertinent coefficient. In particular for head, neck, chest, abdomen



and pelvis, conversion coefficients reported by Deak et al. [17] were used. These coefficients are based on ICRP Publication 103 tissue weighting factors and adult female and male anthropomorphic phantoms that include all the organs and tissues contributing to the effective dose as defined in ICRP Publication 60 and the new organs and tissues not previously considered (the salivary glands, extrathoracic tissue, lymph nodes, prostate, oral mucosa, and the nasal vestibule).

For humera and femura, coefficients evinced from other references were used [20, 21] concerning musculoskeletal studies.

For the segments Head and Neck a further correction factor, experimentally measured, has been used, to account for the ratio  $nCTDI_{w16}/nCTDI_{w32}$ , the numerator and the denominator of the fraction being the normalized weighted dose indexes related to the phantoms of diameter 16 and 32 cm, respectively. In such a way the contribution to the effective dose due to the irradiation of these two anatomical regions is evaluated with a more appropriate geometry. In fact, the arms positioned over the head do not compensate for the minor diameter effectively.

First, sex-averaged conversion coefficients were used. Then sex-specific conversion factors were considered [17]. Finally, correction for the body weight factor was done to account for patient body weight differences with respect to the reference human phantoms (73 and 58 kg for male and female phantom, respectively). In this way the dose evaluation is tailored to individual patient body segment lengths and body masses, allowing for a better approximation to be achieved [22, 23].

#### CT scanner tests

The following points were also evaluated: (a) the accuracy of the nominal value of the  $CTDI_{vol}$  produced by the scanner; (b) the gain in noise reduction achieved using the iterative reconstruction algorithm iDose, installed in the scanner Philips Brilliance 64—such a parameter was evaluated considering the standard deviation of the pixel signal, expressed in Hounsfield Units (HU) in a region of interest of the image of a phantom; (c) the MTF. For point (a) a pencil beam dosimeter UnforsXi and a cylindrical phantom with diameter of 32 cm simulating the body geometry were used; for points (b) and (c) the Catphan phantom was used; in particular the homogeneous section and the section containing the set of bar patterns with different spatial frequency were used, respectively, for noise and MTF evaluation. Images obtained with and without the iDose option were compared for the same protocol WBLDMDCT. MTF was evaluated using the Droege method [24] using the points ranging from the maximum value to 1/10 of it.

## Conventional X-ray examination

### Conventional X-ray imaging protocol

In order to evaluate the dose imparted to the patient during the conventional X-ray examination, a Rando phantom was exposed, using the imaging protocol that was previously employed with patients, including: skull (anterior–posterior AP and lateral LAT projections), cervical spine (AP and LAT), dorsal spine (AP and LAT), lumbar spine (AP and LAT), pelvis (AP), ribs (AP, oblique and AP inferior), humera (AP) and femura (proximal and distal AP). Some of the images of the Rando acquired with this protocol are shown in Fig. 1B. Since a Rando phantom does not have humera or femura, data concerning these segments were obtained from patients' examinations stored in the local data base.

The images were acquired using the automatic control of exposure, as is done in a clinical setting.

The equipment used for the investigation is a remote controlled GMM Opera, with digital detector FPD Pixium RAD4343, pixel size 148  $\mu\text{m}$ .

### Conventional X-ray dose index

The dose descriptor used here for conventional radiography is the free-in-air Dose Area Product (DAP [ $\text{mGy} \times \text{cm}^2$ ]). It accounts for both the intensity and the size of the beam from an X-ray tube. This physical quantity is easily measured by a large-area transmission ionization chamber, positioned in correspondence to the diaphragm of the X ray tube. It has been demonstrated that it is a valuable tool for routine dose measurements and somatic risk assessment [25].

### Conventional X-ray effective dose evaluation

A practical way to estimate the effective dose  $E$  during conventional X-ray examinations is based on measured DAP values and DAP-to- $E$  conversion coefficients.

The effective dose of a single radiograph ( $E_{R,p}$ ) is estimated as the product of the  $DAP_{R,p}$  recorded during the radiograph by the DAP-to- $E$  conversion coefficient (taken from literature):

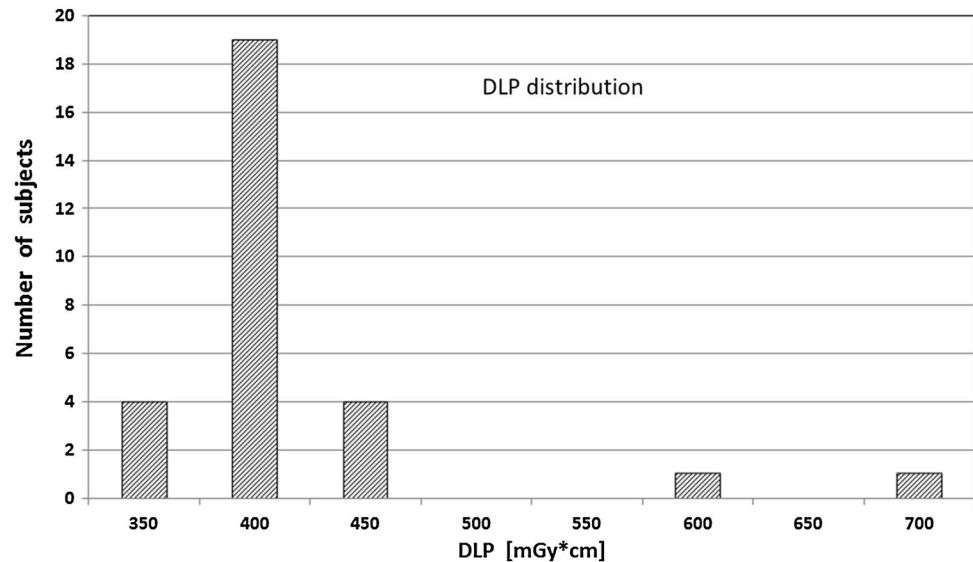
$$E_{R,p} = DAP_{R,p} \times (E/DAP)_{R,p},$$

where R and p indicate the anatomic region irradiated and the view, respectively [the conversion coefficient  $(E/DAP)_{R,p}$  represents the effective dose per unit DAP ( $\text{mSv}/\text{Gy} \times \text{cm}^2$ )].

The effective dose of the complete examination is

$$\sum_{R,p} DAP_{R,p} \times \left( \frac{E}{DAP} \right)_{R,p}.$$

**Fig. 2** Distribution of the DLP values expressed in  $\text{mGy} \times \text{cm}$



The DAPs in the sum are those recorded while exposing the phantom Rando.

## Results

### CT-subjects dose data

The  $\text{CTDI}_{\text{vol}}$  for the protocol in use was equal to 2.62 mGy at 120 kV and 3.88 at 140 kV. Only two large male subjects were studied at 140 kV. The dose indexes, shown in the dose report, are related to the cylindrical phantom of 32 cm of diameter. An example of the dose report is shown in Fig. 1A-h. The contributions to the patient dose due to both survey and diagnostic scan have been considered.

The histogram shown in Fig. 2 represents the distribution of the DLP values of all subjects.

The mean DLP is 398  $\text{mGy} \times \text{cm}$  (value obtained by averaging across all subjects). If data are separated by sex and kV, 397 and 368  $\text{mGy} \times \text{cm}$  are obtained for males and females, respectively, at 120 kV, whereas 628  $\text{mGy} \times \text{cm}$  is the mean DLP at 140 kV. Table 2 summarizes these results.

The mean lengths of the anatomical segments considered are shown in Table 3. The values are similar to those reported by Deak et al. [17] for the adult antropomorphic phantoms, male and female, considered in the above mentioned work.

Based on the DLP values summarized in Table 2 and Fig. 2, patients' anatomical segment lengths and conversion coefficients, effective doses ( $E$ ) were obtained. First, sex-averaged conversion coefficients were used; the results of the estimation are shown in the 4th column of Table 4. The correction factor for Head and Neck geometry was included, producing on average an increase of less than 6 % in the estimated effective doses, with respect to the values

**Table 2** In this table the mean values of the WBLDMDCT DLPs are shown, separated by patient sex (M stands for males and F for females) and X-ray tube high voltage (27 subjects were scanned at 120 kV and only 2 male subjects were scanned at 140 kV)

MeanDLP All subjects $\text{mGy} \times \text{cm}$	MeanDLP M $\text{mGy} \times \text{cm}$	MeanDLP F $\text{mGy} \times \text{cm}$	kV
398	397	368	120
	628	–	140

The value reported in the 1st column was obtained averaging across all subjects

– No female subject was scanned at 140kV

obtained without the correction factor. The scans performed at 140 kV resulted in an effective dose higher than 5 mSv; a mean value of 3.2 mSv ( $\pm 0.2$  standard deviation) was obtained averaging across subjects scanned at 120 kV.

The distribution (not shown here) of these effective dose values reflects the distribution of DLP values, from which they are derived (Pearson coefficient of correlation equal to 0.98).

Then sex-specific conversion coefficients were used, resulting in the effective dose values shown in the 5th column of Table 4.

Application of sex-specific conversion factors demonstrated changes in distribution of the effective dose values. A further change was also produced by including the patient weight factor [23, 24] (data shown in the 6th column of the Table 4). Patient weight information was available for 26 subjects; the mean ( $\pm$ standard deviation) body weight was  $59.1 \pm 9.7$  and  $83.0 \pm 20.5$  for females and males, respectively. The new dose data show a good inverse correlation with the patient weight data (Pearson

**Table 3** Mean length of the patients' body segments expressed in cm

	<i>L</i> (cm) head	<i>L</i> (cm) neck	<i>L</i> (cm) chest	<i>L</i> (cm) abdomen	<i>L</i> (cm) pelvis	<i>L</i> (cm) femura	<i>L</i> (cm) humera
F	18.68	6.25	19.47	17.33	19.55	36.06	28.12
M	20.00	7.42	21.29	19.09	21.24	41.03	31.47
All	19.32	6.81	20.35	18.18	20.36	38.46	29.74

The values were obtained averaging across female subjects (F), male subjects (M) and all subjects (All)

**Table 4** The dose values, expressed in mSv, are listed for each subject (row 1–29)

Subject #	Sex	Weight (kg)	Effective dose (mSv) (based on sex-averaged CC)	Effective dose (mSv) (based on sex-specific CC)	Effective dose (mSv) (based on sex-specific CC and PWCF)
1	F	49	3.10	3.60	4.26
2	M	84	5.27	4.49	3.91
3	M	85	3.57	3.09	2.65
4	M	80	3.44	2.94	2.68
5	M	86	3.45	3.00	2.55
6	M	54	2.92	2.46	3.33
7	F		2.86	3.32	
8	F	60	3.30	3.83	3.70
9	F		3.21	3.71	
10	M	73	3.21	2.74	2.74
11	M	75	3.27	2.79	2.72
12	F	53	3.04	3.53	3.86
13	F	50	2.96	3.44	3.99
14	F	50	2.93	3.38	3.93
15	F	52	3.10	3.60	4.02
16	M	65	3.19	2.71	3.04
17	F	59	2.97	3.45	3.39
18	F	62	3.16	3.67	3.44
19	F	65	3.25	3.76	3.36
20	F	67	2.97	3.46	2.99
21	M	68	3.31	2.81	3.01
22	M	105	3.76	3.16	2.20
23	M	91	3.59	3.05	2.44
24	F	83	3.29	3.83	2.68
25	M	82	3.26	2.78	2.47
26	F		3.06	3.55	
27	M	140	5.41	4.66	2.43
28	M	74	3.45	2.91	2.87
29	F	60	3.35	3.88	3.75

Sex and weight information are also reported (2nd and 3rd column respectively). The 4th column shows the values obtained using sex-averaged DLP-to-effective dose CC; the 5th column shows the values obtained using sex-specific DLP-to-effective dose CC; the 6th column shows values obtained by using sex-specific DLP-to-effective dose CC and PWCF

CC conversion coefficients, PWCF patient weight correction factor, F female, M male

correlation coefficient equal to  $-0.76$ ). This can be seen in Fig. 3 (effective dose expressed in mSv is represented as a function of patient weight expressed in kg; the grey and black data relate to female and male subjects, respectively).

The fact that female and male populations differentiate with mean effective dose of  $3.6 \pm 0.5$  e  $2.8 \pm 0.4$  for females and males, respectively (effective dose expressed in mSv  $\pm$  standard deviation), is highlighted. The two

**Fig. 3** Patient effective doses (mSv)—obtained using sex-specific DLP-to-effective dose conversion coefficients and patient weight correction factor versus the patient weight. The data show a good inverse correlation (Pearson coefficient  $-0.76$ )

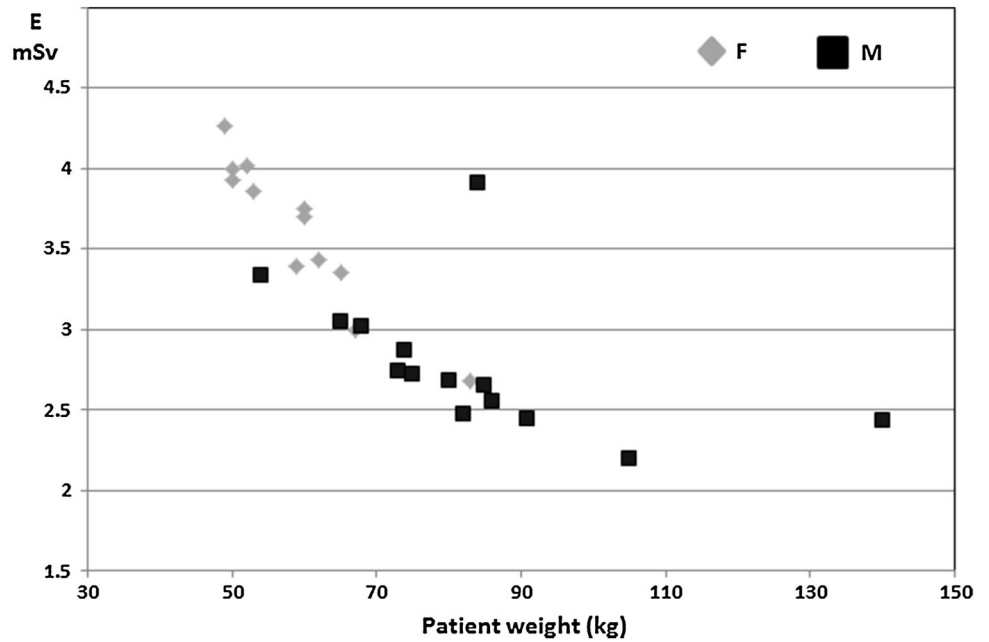
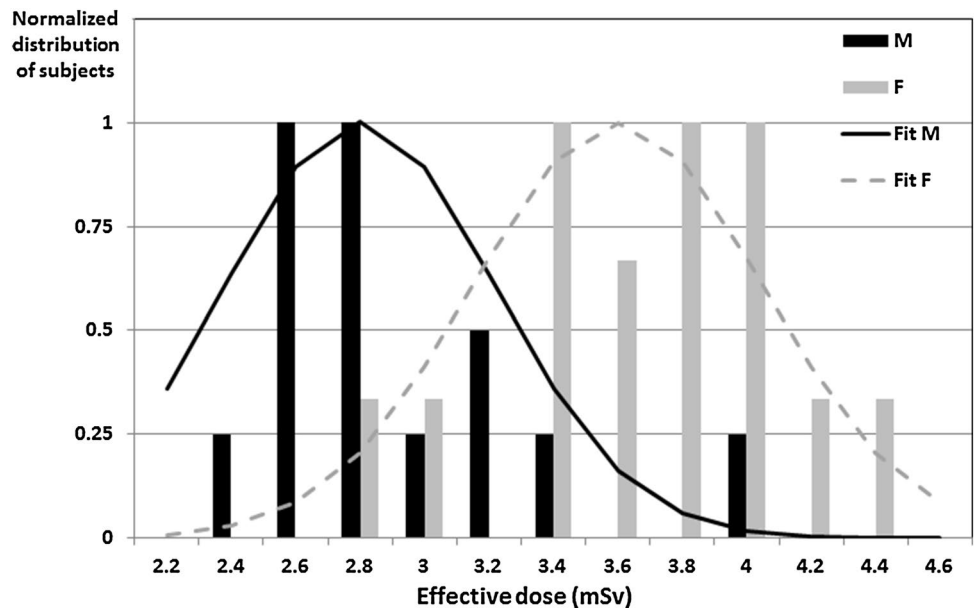


**Fig. 4** The histograms show the effective dose distribution for the two groups of patients, males (*M-black*) and females (*F-grey*). The continuous and dotted lines represent a normal probability function with mean effective dose  $\mu$  and standard deviation  $\sigma$  deduced from experimental data



distributions are shown in Fig. 4. The continuous and dotted lines represent the corresponding probability functions calculated with a normal distribution function  $P_{\mu,\sigma}(E) = \frac{1}{\sigma\sqrt{2\pi}}e^{-\frac{(E-\mu)^2}{2\sigma^2}}$ , having mean value  $\mu$  and standard deviation  $\sigma$  deduced from experimental data.

The distribution parameters (mean value, standard deviation, minimum, maximum, median) are shown in Table 5.

Using the *t* Student test, a value of *p* lower than 0.004 has been obtained for the difference between the two groups.

**CT scanner tests**

The results of the scanner tests performed with phantoms are the following:

- a) Difference between nominal value and measured value of  $CTDI_{vol} < 8 \%$
- b) Noise reduction expressed as the ratio of the standard deviations  $\sigma$  of the pixels of a ROI set in two images reconstructed with and without iDose  $\sigma_{iDose} / \sigma_{no\ iDose} = 0.6$



**Table 5** Patient dose distribution parameters

Effective dose E (mSv)	All subjects (based on sex-averaged CC–no PWCF)	F (based on sex-specific CC)	M (based on sex-specific CC)	F (based on sex-specific CC and PWCF)	M (based on sex-specific CC and PWCF)
Mean value	3.4	3.6	3.1	3.6	2.8
Standard deviation	0.6	0.2	0.6	0.5	0.4
Minimum	2.9	3.3	2.5	2.7	2.2
Maximum	5.4	3.9	4.7	4.3	3.9
Median	3.4	3.6	2.9	3.7	2.7

Mean effective dose, standard deviation, minimum, maximum and median values are shown. 1st column: values obtained using sex-averaged DLP-to-effective dose CC for all subjects; 2nd column: values obtained using sex-specific DLP-to-effective dose CC—female group; 3rd column: values obtained using sex-specific DLP-to-effective dose CC—male group; 4th column: values obtained using sex-specific DLP-to-effective dose CC and PWCF—female subjects; 5th column: values obtained using sex-specific DLP-to-effective dose CC and PWCF—male subjects  
CC conversion coefficients, PWCF patient weight correction factor, F females, M males

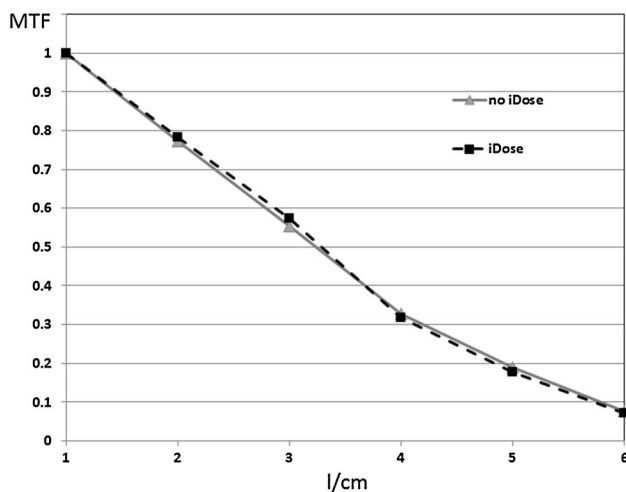


**Fig. 5** Comparison of the MTF measured for two images, obtained with and without the iDose algorithm, respectively, using the same scan and reconstruction parameters. Catphan Phantom and Droege method, were used. The two curves overlap (difference < 1.7 %). Abscissa lines per centimetre

- c)  $MTF_{iDose} = MTF_{no\ iDose}$  (mean difference for the points considered < 2 %). The two curves are plotted in Fig. 5.

Image-j was used to open and process images.

### Conventional X-ray-Rando dose data

Table 6 shows the DAP values recorded reproducing the conventional protocol for the study of the whole skeleton with the anthropomorphic Rando phantom. The effective dose values obtained for each single image are reported in the same table. The total effective dose is about 1.2 mSv.

The data were analysed using excel sheets.

### Discussion

CT, due to its general high-level dose, has been object of recommendations addressing radioprotection aspects [20] and still remains the main contributor to the collective dose [17, 22, 26]. Also high-level radiation doses are given to organs included in the irradiated volume, but of no interest for the examination, for instance the eye lens during a head CT or the breast during a chest CT.

Several studies have been carried out to estimate the cancer risk related to the CT technique, following the enormous technological development that has favoured the extension of the field of application and also an increasing interest in total body studies [27, 28].

In the case of the WBLDM-DCT the radioprotection problem is reduced by the possibility of obtaining good quality imaging with low dose, thanks to the high intrinsic contrast of bone. An improved image quality is obtained as a consequence of the use of IR that allows image noise reduction, estimated to be 40 % for this protocol, with respect to the image noise that would be measured, for the same dose, using conventional reconstruction. This is in agreement with previous study results [11, 12].

In our study the values of effective dose of WBLDM-DCT protocol ranged from 2.2 to 4.3 mSv, with mean values of 3.6 and 2.8 mSv for females and males, respectively. This difference between males and females has been highlighted using sex-specific conversion coefficients and body weight correction factors. For the same scan parameters, sex-specific conversion coefficients cause an effective dose rise higher by about 16 % on average for females with respect to males, although DLP values are lower for females with respect to males. In fact, conversion coefficients for females are higher than those calculated for males, owing to differences in body size, organ position and organ weighting factors [17]. Substantial differences

**Table 6** Exposure parameters and effective dose data obtained from the simulation of the conventional examination of the whole skeleton carried out with a Rando phantom

Examination	View	Field size 1 (cm)	Field size 2 (cm)	kV	mAs	DAP (mGy × cm <sup>2</sup> )	E/DAP (mSv/Gy × cm <sup>2</sup> )	E (mSv)
Skull	AP	20	30	68	54.0	641	0.06	0.04
Skull	LAT	30	28	65	40.2	568	0.04	0.02
Cervical spine	AP	17	27	68	21.2	192	0.19	0.04
Cervical spine	LAT	20	28	66	18.4	191	0.12	0.02
Dorsal spine	AP	20	40	85	12.5	326	0.24	0.08
Dorsal spine	LAT	20	40	85	32.5	881	0.09	0.08
Lumbar spine	AP	40	19	90	16.6	463	0.22	0.10
Lumbar spine	LAT	20	40	95	33.6	1145	0.09	0.11
Pelvis	AP	35	30	70	59.2	1187	0.14	0.17
Ribs	AP	30	40	75	23.6	698	0.24	0.17
Inferior ribs	AP	29	23	75	38.6	613	0.18	0.11
Ribs	OBLR	40	40	75	19.8	713	0.13	0.09
Ribs	OBLL	40	40	75	26.4	943	0.13	0.12
Humera	AP (R + L)			75	3.0	55	0.06	0.01
Proximal femura	AP (R + L)			75	17.2	226	0.04	0.02
Distal femura	AP (R + L)			75	14.0	184	0.04	0.01
							Total	1.18

Each row concerns a single radiography image. 1st column: body region imaged; 2nd column: kind of view; 3rd and 4th columns: beam size; 5th and 6th columns: exposure parameters (kV and mAs); 7th column: DAP; 8th column: DAP-to-*E* conversion coefficient [mSv/Gy × cm<sup>2</sup>]; 9th column: estimated effective dose *E* [mSv]

AP anterior–posterior, LAT lateral, OBL oblique, L left, R right

concern chest, abdomen and pelvis coefficients, whereas head and neck coefficients are very similar for males and females.

Body weight factors cause dose decrease for subjects with body weight greater than those of the reference phantom and dose increase for subjects with body weight lower than those of the reference phantom [22, 23]. In our study, the inclusion of the weight factor has produced a further increase of the difference between males and female from 16 to 28 %, due to a higher body weight of the males with respect to the male reference phantom (on average +10 kg), with a consequent dose decrease.

Behind this inter and intra gender variability, the dose values estimated in our institution are consistent with data reported in literature. These values are lower than those due to a traditional CT investigation of a single segment like chest or abdomen, with typical dose values ranging from 6 to 15 mSv [29].

In our study the effective dose estimated for the “reference male” was 3.1 mSv, that is about 2.5-fold higher than the dose of the corresponding conventional X ray study. Nevertheless, the advantages of the CT technique with respect to the conventional X ray to study MM patients’ skeleton have been assessed in several studies [2, 5–7, 30]. It depends on the intrinsic features of the technique: the high spatial and contrast resolution, the absence of

interposition in the evaluation of complex anatomical structure, such as spine, pelvis and ribs, the ability to depict simultaneously extraosseous localizations of the disease. Furthermore, coronal, sagittal and oblique reconstructions (MPR) are of great value.

In our experience too the superiority of the CT examination was well demonstrated. Owing to its better spatial and contrast resolution, CT allowed the detection of small skull, vertebral and pelvic lesions undetectable or easily overlooked in X-ray examinations (Fig. 6A-a–d).

In addition, endomedullary and extraosseous nodules were easily recognized (Fig. 6A-e, f).

Moreover in our population, WBLDMDCT assessed several incidental findings, especially thoracic abnormalities. They have been mentioned in the report. Most of them did not have a clinical impact; nevertheless, in two cases a prompt diagnostic/therapeutic workup was elicited (Fig. 6B). Overall, in agreement with the above mentioned authors, we also found such an improvement in diagnostic accuracy of CT examination to justify the dose increment.

Also significant advantages are achieved for the patient, usually elderly and suffering from bone pain.

Another favourable aspect is represented by the age of the subjects undergoing this protocol. In fact, the stochastic risk decreases with increasing age, in elderly people (≥70 years) about 10 times lower than in paediatric population



**Fig. 6** **A** Axial CT images nicely depict small lytic lesions within the skull (*a*), in the pelvis (*b*), in a thoracic vertebra and the adjacent rib (*c*), undetectable or easily overlooked in a X-ray examination; reformatted sagittal CT image shows numerous lytic lesions and multiple compression fractures in the thoracic and lumbar spine (*d*); reformatted coronal CT image shows an endomedullary soft tissue nodule

in the humerus with minimal scalloping (*e*); axial CT image shows a huge solid mass destroying the thoracic vertebra and the rib and extending in the adjacent soft tissue of the thoracic apex (*f*). **B** Incidental finding: a 16 mm left pulmonary nodule (*g*) and a right lower lobe apical segment consolidation (*h*)

[31]. The risk averaged across the whole population is about  $5 \times 10^{-5} \text{ mSv}^{-1}$  [15].

In terms of economic cost, a rough estimation indicated that the two methods are equivalent.

Then, on the whole, the adoption of the WBLDMDCT as an alternative to conventional radiography is advantageous.

## Conclusions

The effective dose evaluated for the WBLDMDCT protocol recently adopted in our institution has shown to be on average 3.2 mSv, a little bit lower than the values reported in previous studies, with a difference between males and females due to sex-specific conversion factors and body weight factor that cause in the latter on average a dose increase of about 28 % than that for the former. Considering the mean value obtained for the standard male, the effective dose is about 2.5 times the dose evaluated for the examination of the skeleton “in toto” based on conventional method. Taking into account the advantages of the WBLDMDCT in terms of image quality, patient comfort and patient age, it can be concluded that on balance the adoption of this diagnostic imaging method is positive.

**Acknowledgments** The authors acknowledge Luisella Gnani and Pierluigi Rizzi for help with data collection and image quality tests of the scanner.

## Compliance with ethical standards

**Conflict of interest** The authors declare that they have no conflict of interest.

**Statement of human rights** Ethical approval: “All procedures performed in studies involving human participants were in accordance with the ethical standards of the institutional and/or national research committee and with the 1964 Helsinki declaration and its later amendments or comparable ethical standards.”

**Informed consent** For this type of study formal consent is not required.

## References

1. Delorme S, Baur-Melnyk A (2009) Imaging in multiple myeloma. *Eur J Radiol* 70:401–408. doi:10.1016/j.ejrad.2009.02.005
2. Kim SH, Smith SE, Mulligan ME (2011) Hematopoietic tumors and metastases involving bone. *Radiol Clin N Am* 49:1163–1183. doi:10.1016/j.rcl.2011.07.004
3. Baur-Melnyk A, Reiser M (2008) Oncohaematologic disorders affecting the skeleton in the elderly. *Radiol Clin N Am* 46:785–798. doi:10.1016/j.rcl.2008.05.002
4. Horger M, Claussen CD, Bross-Bach U, Vonthein R, Trabold T, Heuschmid M, Pfannenbergl C (2005) Whole-body low-dose multidetector row-CT in the diagnosis of multiple myeloma: an alternative to conventional radiography. *Eur J Radiol* 54:289–297. doi:10.1016/j.ejrad.2004.04.015
5. Horger M, Pereira P, Claussen CD, Kanz L, Vonthein R, Denecke B, Driessen C (2008) Hyperattenuating bone marrow abnormalities in myeloma patients using whole-body non-enhanced low-dose MDCT: correlation with haematological parameters. *Br J Radiol* 81:386–396. doi:10.1259/bjr/21850180
6. Gleeson TG, Moriarty J, Shortt CP, Gleeson JP, Fitzpatrick P, Byrne B, McHugh J, O’Connell M, O’Gorman P, Eustace SJ (2009) Accuracy of whole-body low-dose multidetector CT (WBLDCT) versus skeletal survey in the detection of myelomatous lesions, and correlation of disease distribution with whole-body MRI (WBMRI). *Skelet Radiol* 38:225–236. doi:10.1007/s00256-008-0607-4
7. Ippolito D, Besostri V, Bonaffini PA, Rossini F, Di Lelio A, Sironi S (2013) Diagnostic value of whole-body low-dose computed tomography (WBLDCT) in bone lesions detection in patients with multiple myeloma (MM). *Eur J Radiol* 82:2322–2327. doi:10.1016/j.ejrad.2013.08.036
8. Decreto Legislativo n. 187 (2000) Attuazione della direttiva 97/43/EURATOM in materia di protezione sanitaria delle persone contro i pericoli delle radiazioni ionizzanti connesse ad esposizioni mediche
9. European Commission (2012) Radiation protection N. 162 criteria for acceptability of medical radiological equipment used in diagnostic radiology. *Nucl Med and Radiother*. doi:10.2768/22561
10. Beister M, Kolditz D, Kalender WA (2012) Iterative reconstruction methods in X-ray CT. *Physica Med* 28:94–108. doi:10.1016/j.ejmp.2012.01.003
11. Ghetti C, Ortenzia O, Serreli G (2012) CT iterative reconstruction in image space: a phantom study. *Physica Med* 28:161–165. doi:10.1016/j.ejmp.2011.03.003
12. Pontana F, Pagniez J, Flohr T, Faivre JB, Duhamel A, Remy J, Remy-Jardin M (2011) Chest computed tomography using iterative reconstruction vs filtered back projection (Part 1): evaluation of image noise reduction in 32 patients. *Eur Radiol* 21:627–635. doi:10.1007/s00330-010-1990-5
13. AAPM Task Group 23 (2008) The measurement, reporting and management of radiation dose in CT. AAPM Report n. 96. ISBN: 978-1-888340-73-0
14. ICRP (1996) Conversion coefficients for use in radiological protection against external radiation. Publication 74. *Ann. ICRP* 26(3–4). ISBN 0 08 042739 1
15. ICRP The 2007 Recommendations of the International Commission on Radiological Protection. ICRP publication 103. *Ann ICRP* 2007; 37(2–4):1–332
16. Hart D, Wall BF (2011) Radiation exposure of the UK population from medical and dental X-ray examinations. *NRPB-W4*. ISBN 0 85951 468 4
17. Deak PD, Smal Y, Kalender WA (2010) Multisection CT protocols. Sex- and age-specific conversion factors used to determine effective dose from dose-length product. *Radiology* 257(1):158–166. doi:10.1148/radiol.10100047
18. Huda W, Ogden KM, Khorasani MR (2008) Converting dose-length product to effective dose at CT. *Radiology* 248(3):995–1003. doi:10.1148/radiol.2483071964
19. International Commission on Radiation Protection (2007) Managing patient dose in multi-detector computed tomography (MDCT). ICRP publication 102 *Ann ICRP*; 37(1):1–79. doi:10.1016/j.icrp.2007.08.006
20. Biswas D, Bible JE, Bohan M, Simpson AK, Jonathan PG, Whang PG, Grauer JN (2009) Radiation exposure from musculoskeletal computerized tomographic scans. *J Bone Joint Surg* 91:1882–1889. doi:10.2106/JBJS.H.01199
21. Henckel J, Richards R, Lozhkin K, Harris S, Rodriguez y Baena FM, Barrett ARW, Cobb JP (2006) Very low dose computed tomography for planning and outcome measurement in

- knee replacement. *J Bone Joint Surg* 88-B(11):1513–1518. doi:[10.1302/0301-620X.88B11.17986](https://doi.org/10.1302/0301-620X.88B11.17986)
22. Huda W, Mettler FA (2011) Volume CT dose index and dose-length product displayed during CT: what good are they? *Radiology* 258(1):236–242. doi:[10.1148/radiol.10100297/-DC1](https://doi.org/10.1148/radiol.10100297/-DC1)
  23. Huda W, Gkanatsios NA (1997) Effective dose and energy imparted in diagnostic radiology. *Med Phys* 24(8):1311–1316
  24. Droegge RT, Morin RL (1982) A practical method to measure the MTF of CT scanners. *Med Phys* 9(5):758–760
  25. Shrimpton PC, Wall BF, Jones DG, Fisher ES (1984) The measurement of energy imparted to patients during diagnostic X-ray examinations using the Diamentor exposure-area product meter. *Phys Med Biol* 29(10):1199–1208
  26. Wiest PW, Loeken JA, Heintz PH, Mettler FA Jr (2002) CT scanning: a major source of radiation exposure. *Semin Ultrasound CT MRI* 23(5):402–410. doi:[10.1016/S0887-2171\(02\)90011-9](https://doi.org/10.1016/S0887-2171(02)90011-9)
  27. Brenner DJ, Elliston CD (2004) Estimated radiation risks potentially associated with full-body CT screening. *Radiology* 231:440–445. doi:[10.1148/radiol.2323031095](https://doi.org/10.1148/radiol.2323031095)
  28. de Gonzalez AB, DPhil, Mahesh M, MS, PhD, Kim K-P, PhD, Bhargavan M, PhD, Lewis R, MPH, Mettler F, MD, Land C, PhD (2009) Projected cancer risks from computed tomographic scans performed in the United States in 2007. *Arch Intern Med* 169(22):2071–2077. doi:[10.1001/archinternmed.2009.440](https://doi.org/10.1001/archinternmed.2009.440)
  29. Mettler FA, Huda W, Yoshizumi TT, Mahech M (2008) Effective doses in radiology and diagnostic nuclear medicine: a catalog. *Radiology* 248:254–263. doi:[10.1148/radiol.2481071451](https://doi.org/10.1148/radiol.2481071451)
  30. Mahnken AH, Wildberger JE, Gehbauer G, Schmitz-Rode T, Blaum M, Fabry U, Gunther RW (2002) Multidetector CT of the spine in multiple myeloma: comparison with MR imaging and Radiography. *AJR* 178:1429–1436. doi:[10.2214/ajr.178.6.1781429](https://doi.org/10.2214/ajr.178.6.1781429)
  31. Wall BF, Haylock R, Jansen JTM, Hillier MC, Hart D, Shrimpton PC (2011) Radiation risks from medical X-ray examinations as a function of the age and sex of the patient HPA-CRCE-028. ISBN 978-0-85951-709-6